

# Single spin optical *read-out* in CdTe/ZnTe quantum dot studied by photon correlation spectroscopy

J. Suffczyński,\* K. Kowalik, T. Kazimierczuk, A. Trajnerowicz,  
M. Goryca, P. Kossacki, A. Golnik, M. Nawrocki, and J. A. Gaj  
*Institute of Experimental Physics, University of Warsaw, Hoża 69, 00-681 Warsaw, Poland*

G. Karczewski  
*Institute of Physics, Polish Academy of Sciences, Al. Lotników 32/64, 02-668 Warsaw, Poland*

Spin dynamics of a single electron and an exciton confined in CdTe/ZnTe quantum dot is investigated by polarization-resolved correlation spectroscopy. Spin memory effects extending over at least a few tens of nanoseconds have been directly observed in magnetic field and described quantitatively in terms of a simple rate equation model. We demonstrate an effective (68%) all-optical *read-out* of the single carrier spin state through probing the degree of circular polarization of exciton emission after capture of an oppositely charged carrier. The perturbation introduced by the pulsed optical excitation serving to study the spin dynamics has been found to be the main source of the polarization loss in the read-out process. In the limit of low laser power the *read-out* efficiency extrapolates to a value close to 100%. The measurements allowed us as well to determine neutral exciton spin relaxation time ranging from  $3.4 \pm 0.1$  ns at  $B = 0$  T to  $16 \pm 3$  ns at  $B = 5$  T.

PACS numbers: 78.55.Et, 73.21.La, 78.67.-n, 78.47.+p, 42.50.Dv

## I. INTRODUCTION

One of the consequences of energy quantization in semiconductor quantum dots (QDs) is the suppression of spin relaxation of confined carriers and excitons.<sup>1,2</sup> Recent experiments conducted on ensemble of III-V QDs have demonstrated that electrons confined in the QDs preserve their spin polarization over microsecond<sup>3,4</sup> or even millisecond timescales.<sup>5</sup> It has been also shown, that spin of the electron confined in the QD can be effectively optically *read* and *written*.<sup>5,6,7,8</sup> These features, complementing the fact that individual QDs can be used as non-classical light sources<sup>9,10</sup> make QDs very attractive for implementation in the developing field of quantum information,<sup>11,12</sup> where polarization-encoded single photons would be utilized. However, several difficulties need to be overcome in order to achieve effective operation of quantum qubits based on single QDs. One of them is native QD anisotropy, which does not influence the spin state of a single electron, but determines the eigenfunctions of exciton and induces linear polarization of its emission. Thus, even if the spin of the carrier is effectively stored, it can not be effectively *read*. The polarization of exciton which is formed in the optical *read-out* of the carrier spin state<sup>5</sup> will be determined by the anisotropy. A lot of effort has been devoted to development of fabrication technique enabling creation of QDs possessing no anisotropy,<sup>13</sup> however no straightforward method has been established so far.

In this work single carrier spin memory effects are studied by correlation spectroscopy technique. Description of the experimental results with a simple rate equation model allowed us to determine the degree of the carrier spin polarization conserved in the process of optical *read-out*. We quantify the impact of biexciton formation on

the loss of the carrier polarization memory. We determine also neutral exciton ( $X$ ) spin relaxation time - serving as a one of the model parameters.

The paper is organized as follows. Section II provides information on the sample studied and the experimental setup. Experimental results are collected in Sec. III, which is divided in three parts. A summary of standard cw microphotoluminescence ( $\mu$ -PL) characterization of the sample (Sec. III A) is followed by results of polarized biexciton-exciton ( $XX$ - $X$ ) crosscorrelation measurements (Sec. III B), supplying information on  $X$  spin relaxation time. Charged exciton-neutral exciton ( $CX$ - $X$ ) polarized crosscorrelation experiments reveal single carrier spin memory through effective optical *read-out* (Sec. III C). Section IV contains the rate equation model description of the experimental data.

## II. SAMPLE AND EXPERIMENTAL SETUP

Detailed macro- and micro-PL characterization of the sample used in this work has been presented in Refs. 14, 15, 16. The sample contains a single layer of QDs, self assembled out of two monolayers of CdTe, embedded between ZnTe barriers. Typical density of the QDs is  $10^{12} \text{ cm}^{-2}$ .<sup>17</sup>

The sample was mounted directly on the front surface of a mirror type microscope objective<sup>18</sup> (numerical aperture = 0.7, spatial resolution  $\sim 0.5 \mu\text{m}$ ) and cooled down to  $T = 1.7$  K in a pumped helium cryostat with a superconducting coil. Microphotoluminescence was excited non-resonantly (above the barrier band gap) with short ( $< 1$  ps)  $\text{Ti}^{3+}:\text{Al}_2\text{O}_3$  laser pulses, delivered every 6.6 ns at wavelength of 400 nm (after frequency doubling). The excitation beam was linearly polarized.

Photon correlations were measured in a Hanbury-Brown and Twiss<sup>19</sup> (HBT) type setup with spectral filtering. PL signal arising from the sample was divided in two beams on a polarizing beamsplitter (BS) and directed to the entrances of two grating monochromators (spectral resolution  $200 \mu\text{eV}$ ). The monochromators were tuned to pass photons from a single excitonic transition, chosen independently on each spectrometer. The signals were then detected by two avalanche photodiodes. The diodes were connected to *start* and *stop* inputs of coincidence counting electronics producing histogram (4096 time bins of  $146 \text{ ps}$  each) of correlated counts versus time interval separating photon detection on the first and on the second diode. Total temporal resolution of the setup is estimated at  $1.1 \text{ ns}$ .

Polarization optics (combinations of halfwave and quarterwave retarders with a linear polarizer) implemented in the HBT setup enabled detection of the second-order correlation function for four linear or four circular polarization combinations.

### III. EXPERIMENTAL RESULTS

#### A. Sample characterization

The  $\mu\text{-PL}$  from the QD layer covers the energy range between  $2.20 \text{ eV}$  and  $2.32 \text{ eV}$ . Excitonic transitions studied in this work were selected from the low energy tail ( $2.20 \text{ eV} - 2.24 \text{ eV}$ ) of the  $\mu\text{-PL}$  spectrum, since in this region lines of individual QDs are well resolved and background counts are negligible. Polarization resolved  $\mu\text{-PL}$  spectrum of the QD selected for this study taken at  $B = 0 \text{ T}$  is presented in Fig. 1(a). Dependence of integrated line intensities on excitation power combined with auto- and crosscorrelation data allowed us to identify the observed transitions as neutral exciton ( $X$ ), charged exciton ( $CX$ ) and biexciton ( $XX$ ) recombination.<sup>16</sup> As visible in Fig. 1(a),  $X$  and  $XX$  lines exhibit anisotropic exchange splitting (AES) in two linearly polarized components, resulting from electron-hole exchange interaction in an anisotropic QD.<sup>20</sup>

In order to determine the value of the AES and directions of linear polarizations of the QD emission, energy positions of  $X$ ,  $CX$  and  $XX$  as a function of detection polarization angle were measured (Fig. 2). No energy variation occurs in the case of  $CX$ , in agreement with the expectation (two identical carriers of the trion are in a singlet state). In the case of  $X$  and  $XX$ , oscillations of transition energy are observed with opposite phase and the same amplitude for both lines. For the QD discussed below AES was determined to be  $182 \pm 6 \mu\text{eV}$ .

A common H-V basis of linear polarizations corresponding to QD symmetry axes was determined as rotated  $58^\circ \pm 3^\circ$  from laboratory axes. The QD symmetry axes do not correspond to the main crystallographic axes of the sample, in agreement with previous anisotropy measurements revealing random anisotropy orientation

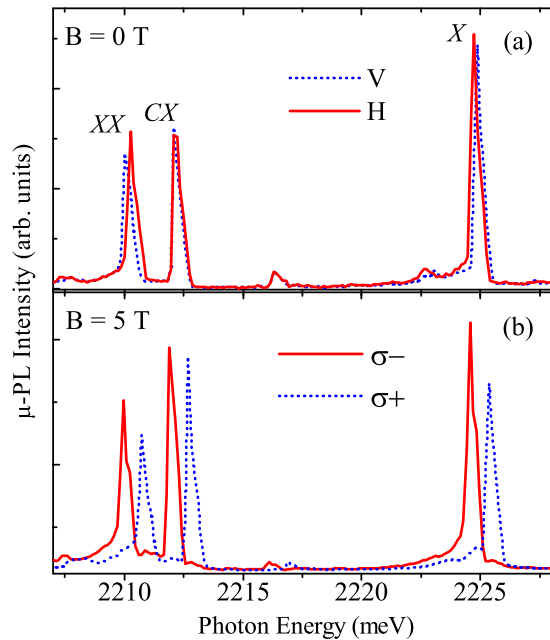


FIG. 1: (Color online) Polarization resolved emission spectra of the selected quantum dot at  $B = 0 \text{ T}$  (a) and  $B = 5 \text{ T}$  (b) detected in linear H-V and circular  $\sigma+/\sigma-$  polarization bases respectively. Excitation at the energy of  $3.1 \text{ eV}$  with the average power  $\sim 0.8 P_{SAT}$  (the saturation power of the X emission  $P_{SAT} = 1.2 \mu\text{W}$  at  $B = 0 \text{ T}$ ).

of CdTe/ZnTe QDs.<sup>15</sup> Determination of the excitonic effective Landé factor based on Zeeman splitting measurements (Fig. 3) performed in magnetic field ranging up to  $5 \text{ T}$  gave approximately the same value  $g = -3.4 \pm 0.1$  for all the three lines. This is expected since the same hole and electron g-factors contribute to the effective g-factor common for all the three excitonic complexes. The determined value is typical for QDs in the investigated sample.<sup>15</sup>

#### B. Polarized XX-X crosscorrelation measurements

In this section, we present time and polarization resolved photon correlations involving biexciton - exciton cascade. The measurements were performed in magnetic field ranging up to  $5 \text{ T}$  and provided an estimate of the  $X$  spin relaxation time. The spin relaxation time was found to increase with magnetic field.

In the experiment, the monochromators were set to detect  $XX$  and  $X$  transition by the *start* and *stop* diode, respectively. The obtained correlation histograms supplied information on relative polarizations of  $XX$  and  $X$  photons emitted subsequently in  $XX$  radiative decay. Due to the pulsed excitation, the histograms consist of peaks spaced equally by the repetition period of the excitation pulses (Fig. 4(a)). The  $XX$ - $X$  crosscorrelation histograms measured at  $B = 0 \text{ T}$  in the linear H-V polarization basis

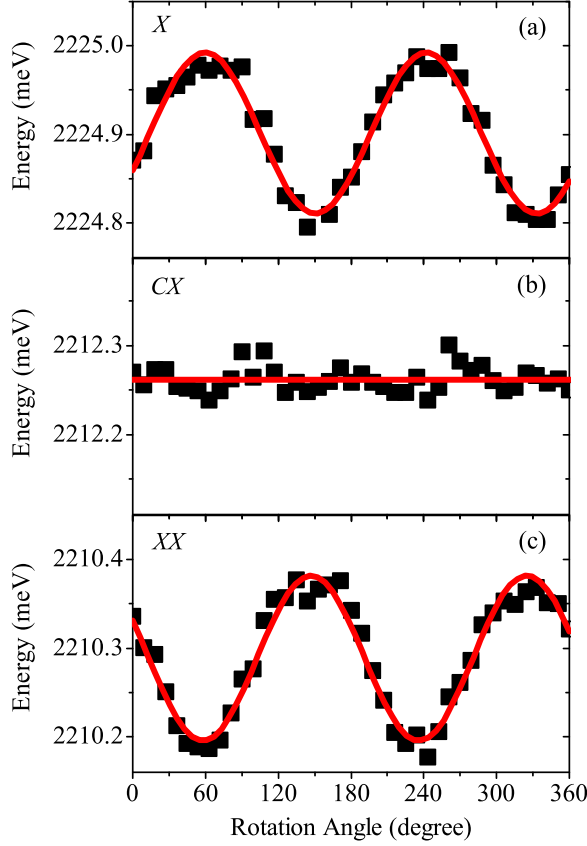


FIG. 2: (Color online) Emission energies of (a)  $X$ , (b)  $CX$  and (c)  $XX$  versus angle of detected linear polarization (points). Solid line represents a sinusoidal fit (a) and (c), or a linear fit (b).

is shown in Fig. 4(a). The normalized areas of the central peak in Fig. 4(a) are  $5.3 \pm 0.4$  and  $5.2 \pm 0.3$  for parallel linear polarizations and  $0.47 \pm 0.02$  and  $0.37 \pm 0.03$  for orthogonal linear polarizations. The measurement repeated in the rotated linear  $-45^\circ/+45^\circ$  polarization basis has not revealed any polarization dependent effects on the zero delay peak (not shown). Similarly, no polarization effects were detected in the measurement performed in circular  $\sigma + / \sigma -$  basis (Fig. 4(b)). Thus,  $XX$  decay produces a pair of classically correlated photons, which is expected for a QD with a reduced symmetry.<sup>21,24,25</sup>

Degree of the correlation in linear H/V polarization basis, estimated following Ref. 21, amounts to  $\chi_{HV} = 0.86 \pm 0.06$ . The nonzero probability of detecting perpendicularly polarized photon pairs originates mostly from the relaxation of excitonic spin occurring over the exciton lifetime. Using the formula derived by Santori *et al.* (Ref. 21) and basing on the  $X$  lifetime ( $\tau_{radX} = 0.29 \pm 0.05$  ns) obtained from an independent experiment performed on the same QD,<sup>16</sup> we estimate  $X$  spin relaxation time at  $T_X = 3.4 \pm 0.1$  ns. The estimated  $T_X$  value is an order of magnitude larger than the excitonic radiative lifetime, in agreement with pre-

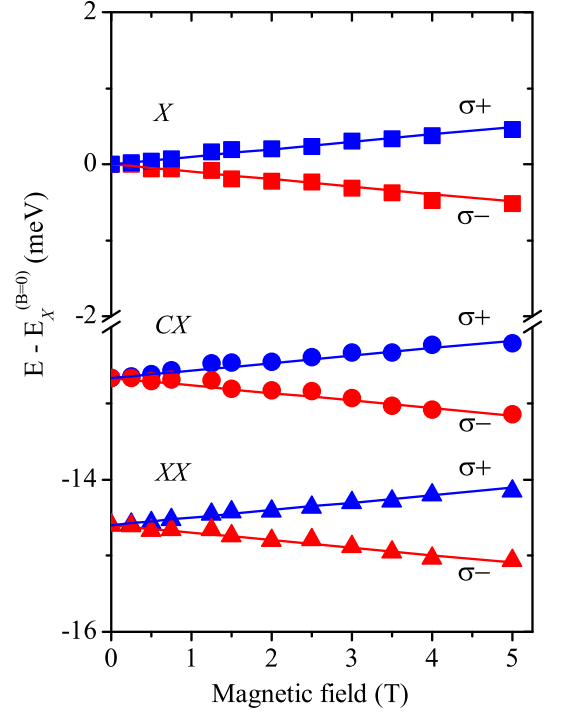


FIG. 3: (Color online) Energy of  $X$ ,  $CX$  and  $XX$  emission relative to zero-field  $X$  energy, measured in both circular polarizations as a function of magnetic field in Faraday configuration. Solid lines represent the calculation of the Zeeman splitting with Landé factor  $g = -3.4$  the same for each line.

vious results obtained on InAs/GaAs<sup>1,21</sup>, CdSe/ZnSe<sup>22</sup> and CdTe/ZnTe<sup>23</sup> QDs.

Mixing of excitonic states with angular momentum  $M = \pm 1$  decreases on application of a magnetic field. It decreases with increasing ratio of the Zeeman splitting to the AES.<sup>26</sup> As the Zeeman splitting becomes dominant, the linearly polarized excitonic doublet observed in  $\mu$ -PL spectra converts in two lines with nearly perfect orthogonal circular polarizations (Fig. 1(b)) corresponding to almost pure  $M = \pm 1$  excitons. A simple calculation<sup>26</sup> provides an estimate of ellipticity of the eigenstates and of the resulting circular polarization degree at 98.3% at  $B = 5$  T. This Zeeman-controlled emission is demonstrated in polarized crosscorrelations measured at  $B = 5$  T on spin split  $XX$  and  $X$  lines in the circular basis (Fig. 4(c)). As seen in Fig. 4(c),  $XX$ - $X$  photon pairs contributing to the central peak exhibit significant, positive (negative) correlation for opposite (equal) circular polarizations, in contrast to the result obtained at  $B = 0$  T (Fig. 4(b)). The respective normalized values of the central peaks in histograms of Fig. 4(c) provide the degree of polarization correlation<sup>21</sup>  $\chi_{\sigma+\sigma-} = 0.95 \pm 0.02$  at  $B = 5$  T. The large degree of polarization correlation (higher than that at zero field) shows that probability of spin-flip accompanied transition between the intermediate excitonic states of the cascade decreases when  $X$  level

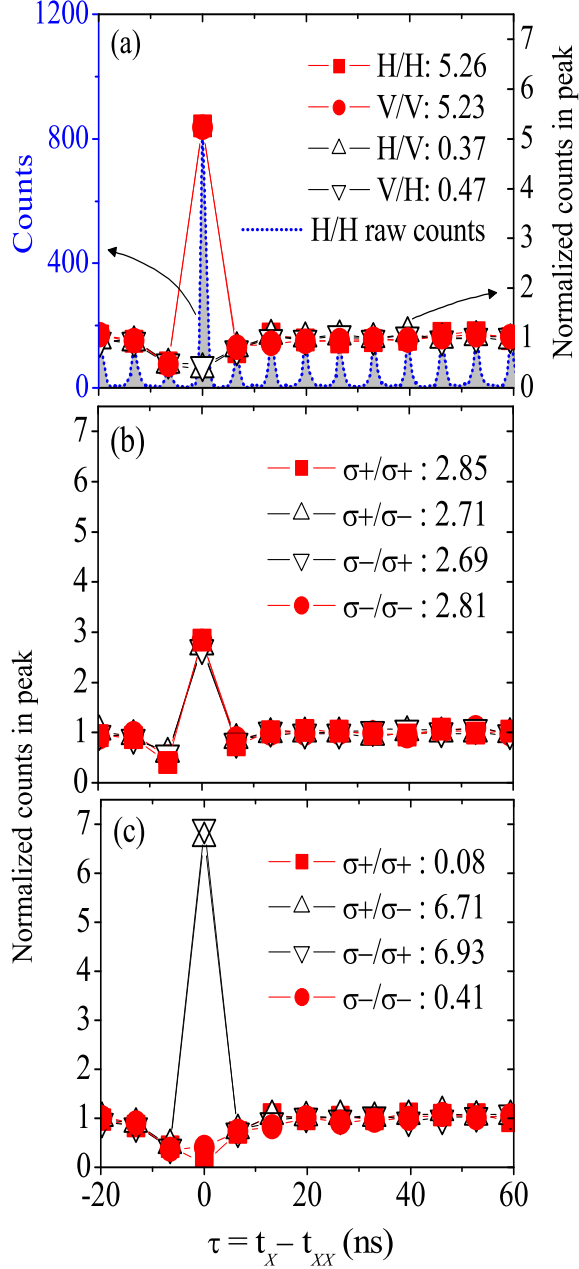


FIG. 4: (Color online) Polarized crosscorrelation of the  $XX$  and  $X$  emission. Each panel contains histograms for four possible polarization combinations of the photon pair. Polarizations of correlated transitions are indicated in  $XX/X$  order. Points represent integrated counts in a peak, normalized to the average value for large delays. Solid lines are guides to the eye. Magnitudes of zero delay peaks in respective histograms are given in the each panel. Polarization correlation of photons from  $XX$ - $X$  cascade is evidenced in linear  $H/V$  polarization basis at  $B = 0$  T (a) and in circular  $\sigma^+/\sigma^-$  polarization basis at  $B = 5$  T (c). There is no polarization correlation in circular  $\sigma^+/\sigma^-$  polarization basis at  $B = 0$  T (b). Panel (a) shows additionally a raw coincidence counts histogram (left axis).

splitting increases in magnetic field. Calculation of the exciton relaxation time at  $B = 5$  T (simple exciton spin-flip time in this case) made under assumption that  $X$  lifetime does not change in the magnetic field<sup>1</sup> and including a correction for incomplete (98.3%) circular polarization of excitonic states, yields the value  $T_X = 16 \pm 3$  ns. This is over four times larger than the value determined for the zero field case. The obtained value will be used as a parameter in the rate equation model introduced in Sec. IV.

In summary, the set of  $XX$ - $X$  crosscorrelations measured (Fig. 4) shows that pairs of photons emitted from an anisotropic QD in  $XX$ - $X$  cascade exhibit at  $B = 0$  T only a strong classical correlation in the linear polarization basis corresponding to symmetry axes of the dot, in agreement with previous experiments.<sup>21,24,25</sup> Anisotropy induced collinear polarization correlation of photons emitted in  $XX$ - $X$  cascade is converted to a counter-circular polarization correlation after applying magnetic field parallel to the sample growth axis. Exciton spin relaxation is found to be slowed down in the presence of magnetic field, as demonstrated by increase of the  $X$  spin relaxation time from  $3.4 \pm 0.1$  ns at  $B = 0$  T to  $16 \pm 3$  ns at  $B = 5$  T.

### C. Single carrier spin memory effects

Previous investigations of QD emission by polarization resolved correlation spectroscopy have been limited to the  $XX$ - $X$  cascade, which was found to produce polarization-correlated<sup>21,24,25</sup> or polarization-entangled<sup>27,28,29</sup> triggered photon pairs. In this section, we present results of time and polarization resolved correlations between charged exciton and neutral exciton photons emitted from a single CdTe/ZnTe QD. We examine the influence of magnetic field on the carrier spin dynamics. The measurements revealed long lasting carrier spin memory in magnetic field and confirmed an effective carrier spin *read-out*.

The measurements were performed in the linear or in the circular polarization basis. The results of  $CX$ - $X$  crosscorrelation involving  $CX$  and  $X$  emission measured at  $B = 0$  T in the circular polarization basis are presented in Fig. 5(a). All the histograms in Fig. 5(a) have their central peak strongly suppressed and exhibit an asymmetric shape, characteristic for  $CX$ - $X$  crosscorrelation. This is known to originate from the QD charge state variation under nonresonant excitation, which favors capture of single carriers instead of entire excitons.<sup>16</sup> The central peak of the  $CX$ - $X$  histogram (Fig. 5) represents the detection of pairs consisting of  $CX$  and  $X$  photons emitted following the same excitation pulse, therefore its suppression reflects expected antibunching of  $CX$  and  $X$  photons. Peaks at a negative (positive) delay represent pairs of photons detected following different pulses, such that  $X$  photon precedes (succeeds)  $CX$  photon. The dependence of circular polarization of  $X$  emission on circular polar-

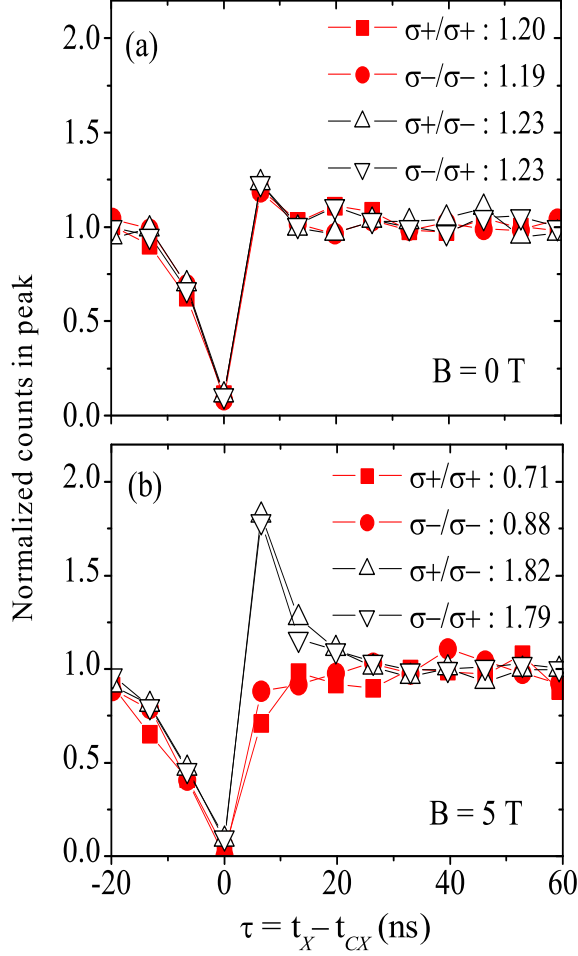


FIG. 5: (Color online) Histograms of  $CX$ - $X$  crosscorrelation measured in the circular  $\sigma + / \sigma -$  polarization basis for four possible combinations of the polarization of the  $CX$ - $X$  photon pair (a) at  $B = 0$  T and at (b)  $B = 5$  T. Polarizations of correlated transitions are indicated in  $CX/X$  order. Points represent integrated and normalized (to the average at large delays) number of counts in a peak. Solid lines are guides to the eye. Values given in panels represent normalized number of counts in  $m = 1$  peak of a respective histogram. Excitation power at  $I_{XX}/I_X = 0.30$  (see Sec. IV). Enhanced  $m = 1$  peaks in the case of correlation between orthogonal  $CX$  and  $X$  polarizations indicate transfer of spin orientation from  $CX$  to  $X$  over time of the repetition period (b).

ization of previously emitted  $CX$  photon ( $m > 0$  peaks) would mean that the spin orientation of the  $CX$  that recombined affects the spin orientation of subsequently formed  $X$ . In such a case the carrier present in the dot after  $CX$  recombination would provide transfer of the spin polarization from  $CX$  to  $X$ . Its spin state would be *read* from the polarization of  $X$  emission. However, no dependence of peak intensity on combination of photon pair polarizations in neither circular (Fig. 5(a)) nor linear H/V (not shown) polarization bases is observed at  $B = 0$  T.

We deduce therefore that polarization of the carrier left in the dot after  $CX$  recombination is not transferred to the  $X$  photon subsequently emitted by the QD. This may be caused by the anisotropic exchange splitting of the  $X$  state, resulting in the averaging out of the circular polarization by precession between two linearly polarized eigenstates. For the same reason, no optical orientation of excitons is observed in anisotropic quantum dots.<sup>30</sup>

However, the polarization transfer becomes significant on application of magnetic field, when both  $CX$  and  $X$  emit in common circular  $\sigma + / \sigma -$  polarization basis. At  $B = 5$  T peaks at small positive delays show a significant enhancement or suppression for opposite or equal circular polarizations, respectively (Fig. 5(b)). The first peak at positive delay ( $m = 1$  peak), represents  $X$  photon detection in the pulse immediately following the detection of  $CX$  photon. Its normalized areas are  $1.8 \pm 0.1$  and  $1.8 \pm 0.1$  for photons of opposite polarization and  $0.88 \pm 0.05$  and  $0.71 \pm 0.05$  for photons of the same polarization. This is an evidence of spin memory in magnetic field.

The intensities of the  $m = 1$  peaks in Fig. 5(b) correspond to polarization degree of 39%. Further ( $m > 1$ ) peaks of the  $CX$ - $X$  histogram also show a polarization, which decreases with increasing peak number. This occurs because each additional excitation pulse reduces the probability that the dot remains in the original, *post CX* recombination, single carrier spin state.

In summary, the results of  $CX$ - $X$  crosscorrelation in magnetic field provide a clear evidence of the polarization memory extending over a few excitation pulses and of effective optical *read-out* of the single carrier spin in the dot.

#### IV. MODEL DESCRIPTION OF THE POLARIZED $CX$ - $X$ CROSSCORRELATION

As already mentioned, the singlet ground state of the charged exciton contains two identical carriers of opposite spins. One of them decays in  $CX$  recombination, emitting a photon with circular polarization determined by its spin. The spin polarization of the second carrier will determine the polarization of an  $X$  photon emitted during  $X$  recombination after next laser pulse. This will happen after trapping a carrier of opposite charge. If the spin polarization is conserved over the repetition period, the  $CX$  and  $X$  photons produced by two consecutive pulses will thus have opposite circular polarizations. In reality, this spin conservation is never perfect and can be measured by polarization correlation coefficient  $P$  defined as

$$P = \frac{I_{\sigma-/ \sigma+} + I_{\sigma+/ \sigma-} - I_{\sigma+/ \sigma+} - I_{\sigma-/ \sigma-}}{I_{\sigma-/ \sigma+} + I_{\sigma+/ \sigma-} + I_{\sigma+/ \sigma+} + I_{\sigma-/ \sigma-}} \quad (1)$$

where  $I_{\gamma/\delta}$  denotes intensity of the correlated counts in the  $CX$ - $X$  histogram measured with  $CX$  and  $X$  photons detected in polarizations  $\gamma$  and  $\delta$ , respectively.



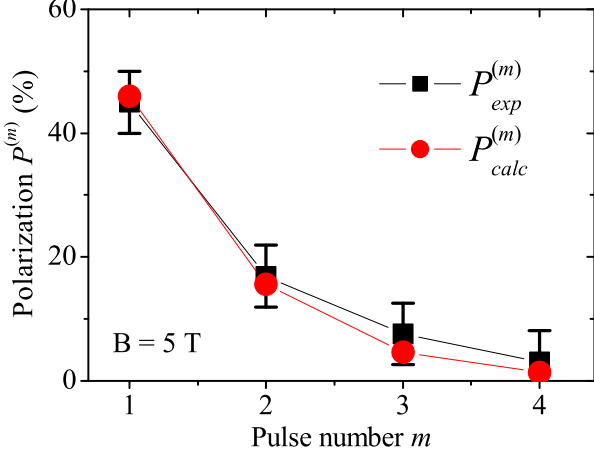


FIG. 6: (Color online) Polarization correlation versus pulse number at  $B = 5$  T. Experimental values (squares) are compared with calculation (dots). Model parameters  $\alpha = 0.71$ ,  $\beta = 0.66$ ,  $\xi = 0.22$ ,  $\kappa = 0.69$  (see text). Excitation power at  $I_{XX}/I_X = 0.26$ . Lines added to guide the eye.

In the experiment we measure  $P_{exp}^{(m)}$  values related to consecutive peaks of the  $CX$ - $X$  histogram, expressed by total correlated counts  $I_{\gamma/\delta}^{(m)}$  of respective peaks, numbered by index  $m$ . Values of  $P_{exp}^{(m)}$  determined for peaks of  $1 \leq m \leq 4$  are shown in Figure 6. The coefficient  $P^{(m)}$  is equivalent to the ratio of the probability that  $X$  photon with polarization defined by the carrier spin conservation is emitted following the  $m$ -th pulse to the overall probability of  $X$  photon emission following the  $m$ -th pulse. Thus,  $P^{(m)}$  can be written taking into account different polarization loss mechanisms. E.g., for  $m = 1$  peak:

$$P_{calc}^{(1)} = \epsilon \frac{n_X^{(1)}}{n_X^{(1)} + n_{XX}^{(1)}} \frac{T_X}{T_X + \tau_{radX}} \kappa \quad (2)$$

where symbols  $n_i^{(m)}$  denote occupation probability of QD states directly after an excitation pulse, which is assumed to be short enough to neglect recombination during excitation (see discussion further below). The upper index given in parentheses encodes the pulse number  $m$ , while the lower index  $i$  encodes the dot state. Factor  $\epsilon$  (in the case of selected QD estimated at 96.2% at  $B = 5$  T) represents the impact of elliptical polarization of the excitonic eigenstate. The fraction with  $XX$  and  $X$  occupation probabilities represents polarization loss due to biexciton recombination channel, where no polarization is transferred by the singlet  $XX$  state. Since  $T_X$  is  $X$  spin-flip time (see Sec. III B), expression  $T_X/(T_X + \tau_{radX})$  represents the loss of the exciton spin polarization during its lifetime. Finally,  $\kappa$  represents other possible loss mechanisms. In particular, it could be a spin-flip of the remaining carrier. However, we checked that magnitude of the peaks in the polarized  $CX$ - $X$  correlation histogram remains unchanged after doubling of the excitation re-

petition period (not shown). This indicates a negligible carrier spin relaxation over the timescale comparable with the repetition period. A possible polarization loss during  $X$  state formation by capture of a second carrier of an opposite charge will be also found negligible (see discussion in the following). Hence, the respective polarization loss results from an interaction of the confined electron with non-equilibrium population of carriers (exchange interaction) and/or phonons (possible local heating of the sample) excited by laser pulses.

The timescale of the observed memory effect might also suggest that  $CX$  recombination leaves in the dot an electron and not a hole. In contrast to the case of the electron, the spin relaxation of the hole is known to be relatively fast,<sup>31</sup> occurring in the time of the order comparable with the repetition period of probing the carrier's spin state in our experiment. Thus, we make tentative assumption that  $CX$  is negatively charged.

We shall also comment on the influence of dark exciton formation on excitonic polarization degree. Dark, non-radiative exciton state is formed in the case when carrier is captured by the dot already containing a carrier of opposite charge and the same spin. After a spin-flip process the dark exciton converts into a bright state and decays radiatively. Such an excitonic luminescence could lower the effective excitonic PL polarization degree. However, the time constant of dark exciton spin-flip is large compared to the excitation repetition period. This is known from the comparison between the results of unpolarized  $CX$ - $X$  crosscorrelation measurements performed with two different repetition periods.<sup>16</sup> They reveal no significant difference in intensity of peaks of the same number in two histograms. Thus, the influence of the dark exciton formation on exciton polarization degree can be neglected and it was not taken into account in the construction of the model describing experimental data.

The measured polarization may be understood as a product of carrier spin polarization reduced by *read-out* efficiency (first two factors in Eq. 2) and loss mechanisms (last two factors in Eq. 2). In order to determine the most prominent factors lowering the measured polarization we introduce a simple rate equation model. It allows us to compute the occupation probabilities necessary for calculation of  $P_{calc}^{(m)}$ . We consider a ladder of states involving five states: from the empty dot to the biexciton state. Since only one charged exciton line of significant intensity is observed, we neglect states of opposite charge (corresponding weak trion line visible in Fig. 1 at 2217 meV). We define a set of variables  $n_0^{(m)}$ ,  $n_e^{(m)}$ ,  $n_X^{(m)}$ ,  $n_{CX}^{(m)}$ ,  $n_{XX}^{(m)}$  describing the occupation of levels (encoded by the lower index) just after the excitation by the  $m$ -th pulse is finished. It is known from independent measurements on the same sample<sup>32</sup> that the effective excitation pulse duration ( $\sim 20$  ps) is much shorter than radiative decay times (hundreds of ps), therefore we neglect recombination during the excitation process. Excitation through capture of single carriers of both signs

and entire excitons with respective time dependent rates  $\alpha(t) = \alpha \cdot f(t)$ ,  $\beta(t) = \beta \cdot f(t)$ , and  $\xi(t) = \xi \cdot f(t)$ , is assumed. A common normalized excitation pulse shape  $f(t)$  is assumed ( $\int_0^{T_{rep}} f(t)dt = 1$ ), while  $\alpha$ ,  $\beta$ ,  $\xi$  represent time-integrated capture rates per pulse. Escape of the carriers out of the dot is not taken into account as it has been shown to be negligible.<sup>16</sup> Our simulations show that within the assumptions of the model, the shape  $f(t)$  of the excitation pulse is not important. We describe the excitation process with the following set of rate equations:

$$\frac{dn_0^{(m)}}{dt} = -(\alpha(t) + \xi(t))n_0^{(m)} \quad (3a)$$

$$\frac{dn_e^{(m)}}{dt} = \alpha(t)n_0^{(m)} - (\beta(t) + \xi(t))n_e^{(m)} \quad (3b)$$

$$\frac{dn_X^{(m)}}{dt} = \xi(t)n_0^{(m)} + \beta(t)n_e^{(m)} - (\alpha(t) + \xi(t))n_X^{(m)} \quad (3c)$$

$$\frac{dn_{CX}^{(m)}}{dt} = \xi(t)n_e^{(m)} + \alpha(t)n_X^{(m)} - \beta(t)n_{CX}^{(m)} \quad (3d)$$

$$\frac{dn_{XX}^{(m)}}{dt} = \xi(t)n_X^{(m)} + \beta(t)n_{CX}^{(m)} \quad (3e)$$

We assume purely radiative decay of excitons. Thus, the initial conditions for a consecutive excitation pulse are determined by the final state of excitonic recombination after preceding excitation pulse. For the particular case of  $m = 1$ , the initial conditions are in a good approximation  $n_e^{(1)}(0) = 1$  and  $n_{i \neq e}^{(1)}(0) = 0$  (single carrier left after  $CX$  recombination present in the dot). Integrated capture rates  $\alpha$ ,  $\beta$ ,  $\xi$  obtained from the experiment on the same QD with no polarization resolution were used.<sup>16</sup> They were scaled by a common factor in order to take into account a variable excitation power. The factor was adjusted to fit the ratio of  $XX$  to  $X$  emission intensity ( $I_{XX}/I_X$ ). (Consistently with Ref. 16,  $\alpha/\beta$  represents capture rate of the first /the second/ carrier to the dot, that is electron /hole/.)

The first consequence of the model is the variation of the calculated polarization coefficient  $P$  with the excitation power. Also the  $P_{exp}^{(1)}$  decreases with the increasing excitation power. This is expected, since the contribution of  $X$  photons coming from  $XX$  radiative decay increases with the excitation intensity. They are effectively unpolarized and they lower the value of  $P_{exp}^{(m)}$ . We determined  $P_{calc}^{(1)}$  for different excitation powers by solving Eqs. 3 with suitably scaled rates  $\alpha$ ,  $\beta$ , and  $\xi$  assuming full conservation of the electron spin ( $\kappa = 1$ ). The Figure 7(a) shows comparison of  $P_{calc}^{(1)}$  for  $\kappa = 1$  and  $P_{exp}^{(1)}$  plotted as a function of the  $I_{XX}/I_X$  ratio. The ratio  $I_{XX}/I_X$

was chosen to represent excitation power, since it provides a convenient measure of excitation intensity. The discrepancy between the experimental and the calculated values is a clear indication that conservation of the electron spin polarization between the  $CX$  and  $X$  emissions is not perfect.

Thus, we fitted  $P_{calc}^{(1)}$  to  $P_{exp}^{(1)}$  with  $\kappa$  being the (only) fitting parameter. Values of  $\kappa$  determined this way are shown in Fig. 7(b) as a function of  $I_{XX}/I_X$  ratio. As visible in the Fig. 7(b),  $\kappa$  attains the value of  $\kappa = 0.69$  at  $I_{XX}/I_X = 0.26$  and decreases with the increasing excitation power. A linear fit to the experimental points is also shown in the Fig. 7(b). The electron polarization conservation, and the electron spin optical *read-out* are almost perfect in the limit of low excitation power.

This means that the capture of the hole to form an exciton with the electron in the QD does not induce any significant polarization loss, since process of  $X$  formation does not depend on excitation power. The dependence of  $\kappa$  on the excitation intensity confirms that  $\kappa$  originates from the factors such as interaction of the confined electron with carriers and/or phonons generated by the excitation pulse, as contribution of these factors depends on the excitation power.

Therefore, the loss of the electron polarization represented by  $\kappa$  takes place following each excitation pulse. This allows us to write down  $P_{calc}^{(m)}$  for consecutive pulses in the form:

$$P_{calc}^{(m)} = (n_e^{(1)})^{m-1} \epsilon \frac{n_X^{(1)}}{n_X^{(m)} + n_{XX}^{(m)}} \frac{T_X}{T_X + \tau_{radX}} \kappa^m \quad (4)$$

The factor  $(n_e^{(1)})^{m-1}$  reflects the probability that QD keeps its one-carrier state unchanged through  $m - 1$  excitation pulses. The factor  $\kappa^m$  represents degree of conservation of the electron spin following  $m$  consecutive excitation pulses. Its exponential dependence on the peak number  $m$  (evidenced by Fig. 6) confirms the role of laser pulses as the source of polarization loss described by  $\kappa$ .

Integration of Eqs. 3 yielded probabilities  $n_i^{(m)}$  of finding the dot in a state  $i$  following  $m$ -th excitation pulse. Thus  $P_{calc}^{(m)}$  for consecutive pulses were calculated from Eq. 4. They are compared with the experimental values of  $P_{exp}^{(m)}$  for peaks of  $1 \leq m \leq 4$  in Fig. 6 for the example case of  $I_{XX}/I_X = 0.26$ . The satisfactory agreement between calculated and experimental values justifies the introduced model.

To summarize this Section,  $CX$ - $X$  crosscorrelation measurements provide evidence for single carrier spin polarization memory in magnetic field. We described quantitatively the polarization memory after consecutive excitation pulses. Comparison between the model and the experiment shows that carrier spin conservation and the optical *read-out* efficiency are close to 100% in the limit of low excitation power. The maximum efficiency of the spin *read-out* obtained in the experiment is 68%. The  $CX$ - $X$  crosscorrelation performed for different excitation

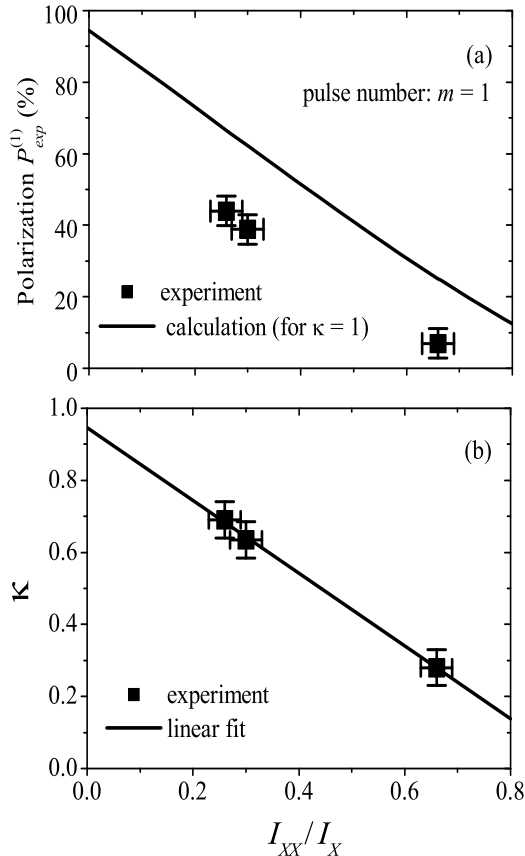


FIG. 7: (a) Polarization correlation at  $B = 5$  T for the first pulse after  $CX$  emission  $P_{exp}^{(1)}$  versus excitation power represented by the ratio  $I_{XX}/I_X$ . Solid line – calculation ( $\kappa = 1$ ) according to Eq. 2. (b) Coefficient  $\kappa$  of carrier spin conservation at  $B = 5$  T determined from fitting of the  $P_{calc}^{(1)}$  to  $P_{exp}^{(1)}$  for different excitation powers.

powers allowed us to verify the expected influence of biexciton formation on the loss of polarization memory.

## V. CONCLUSIONS

We performed polarized crosscorrelation measurements of photons from exciton, biexciton, and trion re-

combination in a single, anisotropic CdTe/ZnTe quantum dot. In absence of magnetic field we observed a strong collinear polarization correlation ( $\chi_{HV} = 0.86 \pm 0.06$ ) of photons emitted in the biexciton-exciton cascade. When Zeeman splitting dominates over anisotropic exchange splitting, the photons in the cascade become correlated in opposite circular polarizations ( $\chi_{\sigma+\sigma-} = 0.95 \pm 0.02$ ). Exciton spin relaxation time values  $T_X = 3.4 \pm 0.1$  ns at  $B = 0$  T and  $16 \pm 3$  ns at  $B = 5$  T were determined from the  $XX$ - $X$  correlation measurements.

Trion-exciton crosscorrelation measurements conducted in magnetic field of 5 T have revealed long timescale (at least tens of ns) polarization memory in the QD excitonic emission. Effective optical *read-out* of the spin polarization of a single carrier confined in the anisotropic QD has been demonstrated in magnetic field. The decay of the polarization memory with the increasing number of excitation pulses separating two correlated photons has been described with a simple rate equation model. It was attributed to the combined influence of competitive biexciton spin singlet recombination and loss of carrier spin polarization, perturbed primarily by the very laser light used for the spin *read-out*. Efficiency of optical *read-out* of the spin in magnetic field turned out to be dependent on the excitation power (the maximum efficiency obtained in the experiment was 68%).

The results obtained indicate CdTe/ZnTe QDs as a valuable proving ground for future applications of polarization controlled single photon emitters or spin qubits in the area of quantum information processing.

## Acknowledgments

This work was partially supported by the Polish Ministry of Science and Higher Education research grants in years 2005-2010 and by European project no. MTKD-CT-2005-029671.

\* Electronic address: Jan.Suffczynski@fuw.edu.pl

<sup>1</sup> M. Paillard, X. Marie, P. Renucci, T. Amand, A. Jbeli, and J. M. Gérard, Phys. Rev. Lett. **86**, 1634 (2001).

<sup>2</sup> A. V. Khaetskii and Y. V. Nazarov, Phys. Rev. B **61**, 12639 (2000).

<sup>3</sup> M. Ikezawa, B. Pal, Y. Masumoto, I. V. Ignatiev, S. Y. Verbin, and I. Y. Gerlovin, Phys. Rev. B **72**, 153302 (2005).

<sup>4</sup> I. A. Akimov, D. H. Feng, and F. Henneberger, Phys. Rev.

Lett. **97**, 056602 (2006).

<sup>5</sup> M. Kroutvar, Y. Ducommun, D. Heiss, M. Bichler, D. Schuh, G. Abstreiter, and J. J. Finley, Nature **432**, 81 (2004).

<sup>6</sup> S. Cortez, O. Krebs, S. Laurent, M. Senes, X. Marie, P. Voisin, R. Ferreira, G. Bastard, J.-M. Gérard, and T. Amand, Phys. Rev. Lett. **89**, 207401 (2002).

<sup>7</sup> A. Ebbens, D. N. Krizhanovskii, A. I. Tartakovskii, F. Pulizzi, T. Wright, A. V. Savelyev, M. S. Skolnick, and



- M. Hopkinson, Phys. Rev. B **72**, 073307 (2005).
- <sup>8</sup> R. J. Young, S. J. Dewhurst, R. M. Stevenson, P. Atkinson, A. J. Bennett, M. B. Ward, K. Cooper, D. A. Ritchie, and A. J. Shields, New J. Phys. **9**, 365 (2007).
  - <sup>9</sup> P. Michler, A. Kiraz, C. Becher, W. V. Schoenfeld, P. M. Petroff, L. Zhang, E. Hu, and A. Imamoglu, Science **290**, 2282 (2000).
  - <sup>10</sup> E. Moreau, I. Robert, J. M. Gerard, I. Abram, L. Manin, and V. Thierry-Mieg, Appl. Phys. Lett. **79**, 2865 (2001).
  - <sup>11</sup> G. Bennet and C. H. Brassard, Proceedings of IEEE Int. Conf. on Computers, Systems and Signal processing, Bangalore, India, 175 (1984).
  - <sup>12</sup> A. K. Ekert, Phys. Rev. Lett. **67**, 661 (1991).
  - <sup>13</sup> D. J. P. Ellis, R. M. Stevenson, R. J. Young, A. J. Shields, P. Atkinson, and D. A. Ritchie, Appl. Phys. Lett. **90**, 011907 (2007).
  - <sup>14</sup> A. Kudelski, K. Kowalik, A. Golnik, G. Karczewski, J. Kossut, and J. A. Gaj, J. Lumin. **112**, 127 (2005).
  - <sup>15</sup> K. Kowalik, A. Kudelski, A. Golnik, J. A. Gaj, G. Karczewski, and J. Kossut, Acta Phys. Pol. A **103**, 539 (2003).
  - <sup>16</sup> J. Suffczyński, T. Kazimierzuk, M. Goryca, B. Piechal, A. Trajnerowicz, K. Kowalik, P. Kossacki, A. Golnik, K. P. Korona, M. Nawrocki, J. A. Gaj, and G. Karczewski, Phys. Rev. B **74**, 085319 (2006).
  - <sup>17</sup> G. Karczewski, S. Maćkowski, M. Kutrowski, T. Wojtowicz, and J. Kossut, Appl. Phys. Lett. **74**, 3011 (1999).
  - <sup>18</sup> J. Jasny and J. Sepioł, Chem. Phys. Lett. **273**, 439 (1997).
  - <sup>19</sup> R. Hanbury-Brown and R. Q. Twiss, Nature **177**, 27 (1956).
  - <sup>20</sup> L. Besombes, K. Kheng, and D. Martrou, Phys. Rev. Lett. **85**, 425 (2000).
  - <sup>21</sup> C. Santori, D. Fattal, M. Pelton, G. S. Solomon, and Y. Yamamoto, Phys. Rev. B **66**, 045308 (2002).
  - <sup>22</sup> T. Flissikowski, A. Hundt, M. Lowisch, M. Rabe, and F. Henneberger, Phys. Rev. Lett. **86**, 3172 (2001).
  - <sup>23</sup> S. Maćkowski, T. A. Nguyen, H. E. Jackson, L. M. Smith, J. Kossut, and G. Karczewski, Appl. Phys. Lett. **83**, 5524 (2003).
  - <sup>24</sup> R. M. Stevenson, R. M. Thompson, A. J. Shields, I. Farrer, B. E. Kardynal, D. A. Ritchie, and M. Pepper, Phys. Rev. B **66**, 081302(R) (2002).
  - <sup>25</sup> S. M. Ulrich, S. Strauf, P. Michler, G. Bacher, and A. Forchel, Appl. Phys. Lett. **83**, 1848 (2003).
  - <sup>26</sup> L. Besombes, L. Marsal, K. Kheng, T. Charvolin, L. S. Dang, A. Wasiela, and H. Mariette, J. Cryst. Growth **214/215**, 742 (2000).
  - <sup>27</sup> R. J. Young, R. M. Stevenson, P. Atkinson, K. Cooper, D. A. Ritchie, and A. J. Shields, New J. Phys. **8**, 29 (2006).
  - <sup>28</sup> R. M. Stevenson, R. J. Young, P. Atkinson, K. Cooper, D. A. Ritchie, and A. J. Shields, Nature **439**, 179 (2006).
  - <sup>29</sup> N. Akopian, N. H. Lindner, E. Poem, Y. Berlatzky, J. Avron, D. Gershoni, B. D. Gerardot, and P. M. Petroff, Phys. Rev. Lett. **96**, 130501 (2006).
  - <sup>30</sup> K. Kowalik, O. Krebs, A. Lemaitre, B. Eble, A. Kudelski, P. Voisin, S. Seidl, and J. A. Gaj, Appl. Phys. Lett. **91**, 183104 (2007).
  - <sup>31</sup> T. Flissikowski, I. A. Akimov, A. Hundt, and F. Henneberger, Phys. Rev. B **68**, 161309(R) (2003).
  - <sup>32</sup> K. Korona, P. Wojnar, J. Gaj, G. Karczewski, J. Kossut, and J. Kuhl, Solid State Commun. **133**, 369 (2005).